Available online at www.sciencedirect.com
ScienceDirect
International Journal of Mass Spectrometry 269 (2008) 165–176
International Journal of Mass Spectrometry
www.elsevier.com/locate/ijms

The remarkable dissociation chemistry of 2-aminoxyethanol ions $NH_2OCH_2CH_2OH^{\bullet+}$ studied by experiment and theory

Karl J. Jobst [a], Paul J.A. Ruttink [b], Johan K. Terlouw [a,*]

[a] *Department of Chemistry, McMaster University, 1280 Main Street West, Hamilton, Ont., Canada L8S 4M1*
[b] *Theoretical Chemistry Group, Department of Chemistry, University of Utrecht, 3584 CH Utrecht, The Netherlands*

Received 11 September 2007; received in revised form 4 October 2007; accepted 9 October 2007
Available online 23 October 2007

Abstract

Low-energy 2-aminoxyethanol molecular ions $NH_2OCH_2CH_2OH^{\bullet+}$ exhibit a surprisingly rich gas-phase ion chemistry. They spontaneously undergo five major dissociations in the microsecond timeframe, yielding ions of *m/z* 61, 60, 46, 32 and 18. Our tandem mass spectrometry experiments indicate that these reactions correspond to the generation of $HOCH_2CH(OH)^+$ (protonated glycolaldehyde), $HOCH_2C(=O)H^{\bullet+}$ (ionized glycolaldehyde), $HC(OH)NH_2^+$ (protonated formamide), $CH_2OH_2^{\bullet+}$ (the methylene oxonium ion) and NH_4^+.

A mechanistic analysis of these processes using the CBS-QB3 model chemistry shows that the molecular ions undergo a 1,4-*H* shift followed by a facile isomerization into the ion–molecule complex $[HOCH_2C(=O)H^{\bullet+}]\cdots[NH_3]$ which acts as the reacting configuration for the five exothermic dissociation processes. Analysis of the D-labelled isotopomer $ND_2OCH_2CH_2OD^{\bullet+}$, in conjunction with our computational results, shows that proton-transport catalysis may be responsible for the partial conversion of the *m/z* 60 glycolaldehyde ions into the more stable 1,2-dihydroxyethene isomer $HOC(H)=C(H)OH^{\bullet+}$.

Keywords: Tandem mass spectrometry; CBS-QB3 model chemistry; Proton-transport catalysis

1. Introduction

Since the first detection of trihalomethanes in drinking water, the qualitative and quantitative characterization of so-called disinfection by-products (DBPs) has become a subject of considerable interest. DBPs are commonly derived from the combination of natural organic matter with disinfection agents like chlorine, chlorine dioxide, ozone and chloramines [1]. Several DBPs have thus far been identified, including trihalomethanes, haloacetic acids, haloacetonitriles, chloral hydrate and cyanogen chloride. It is estimated that these account for approximately 40% of DBPs whereas the remainder are unknown.

In 2001, two unexpected disinfection by-products were reported: the halogenated aminoxyalcohols 1-aminoxy-1-chlorobutan-2-ol and 1-aminoxy-2-bromobutan-2-ol [2]. The structure proposal was based upon a detailed mass spectrometric study involving electron ionization (EI), chemical ionization (CI) and high-resolution data but it remains speculative because little is known about the EI characteristics of aminoxyalcohols.

This prompted us to examine the EI and CI characteristics of 2-aminoxyethanol ($NH_2OCH_2CH_2OH$) as a model compound. In this study we have used tandem mass spectrometry based experiments in conjunction with model chemistry calculations to probe the rich dissociation chemistry of the metastable molecular ions $NH_2OCH_2CH_2OH^{\bullet+}$ (**AE-1**). These ions dissociate via six competing pathways whereas the related 1,2-ethane diol ion $HOCH_2CH_2OH^{\bullet+}$ only loses $HCO^{\bullet}$ in the metastable timeframe [3,4] via a mechanism that features proton-transport catalysis (PTC) [5] in hydrogen-bridged radical cations (HBRCs) [6] as key intermediates. It will be shown that HBRCs also play a key role in the various dissociation reactions of low-energy 2-aminoxyethanol radical cations.

2. Experimental and theoretical methods

The experiments were performed with the VG Analytical ZAB-R mass spectrometer of BEE geometry (B, magnet; E, electric sector) [7] using an electron ionization source

* Corresponding author. Tel.: +1 905 525 9140; fax: +1 905 522 2509.
E-mail address: terlouwj@mcmaster.ca (J.K. Terlouw).

1387-3806/$ – see front matter © 2007 Elsevier B.V. All rights reserved.
doi:10.1016/j.ijms.2007.10.007

at an accelerating voltage of 6–10 kV. Metastable ion (MI) and collision-induced dissociation (CID) mass spectra were recorded in the second field free region (2ffr). In all collision experiments oxygen was used as the collision gas. All spectra were recorded using a PC-based data system developed by Mommers Technologies Inc. (Ottawa). Kinetic energy releases (corrected $T_{0.5}$ values) were measured according to standard procedures [3,8].

The 2-aminoxyethanol sample was synthesized by an established procedure [9] but using *N*,*N*-dimethylformamide rather than dimethyl sulfoxide as the solvent. Its deuterium labelled isotopomer $ND_2OCH_2CH_2OD$ was obtained therefrom by repeated exchange with methanol-OD. The liquid samples were introduced into the source (kept at 120 °C) via a quartz probe inlet. The purity of the (unlabelled) sample and the elemental composition of the major peaks in the 70 eV EI mass spectrum of Fig. 1a was verified by a GC–MS experiment using a Micromass GC-T time-of-flight instrument at its standard mass resolution of 4000–6000 (50% valley definition).

The calculations were performed with the CBS-QB3 model chemistry [10]; for selected species the (computationally much more demanding) CBS-APNO method [11] was also used. Most of the calculations were run with the Gaussian 2003, Rev C.02 suite of programs [12] on the SHARCNET computer network at McMaster University. In the CBS-QB3 model chemistry the geometries of minima and connecting transition states are obtained from B3LYP density functional theory in combination with the 6-311G (2d,d,p) basis set (also denoted as the CBSB7 basis set). The resulting total energies and enthalpies of formation for minima and connecting transition states (TS) in 2-aminoxyethanol systems of ions are presented in Table 1. A selection of the optimized geometries is presented in Fig. 2. The estimated reliability of the CBS-QB3 derived enthalpies is ± 2 kcal mol^{-1} for minima and ± 4 kcal mol^{-1} for transition state structures [13]. Computational data pertaining to the dissociation products are found in Table 2. Spin contaminations ($\langle S^2 \rangle$ values of Table 1) were acceptable. Unless stated otherwise, all enthalpies presented in the text and in the schemes (numbers in square brackets) refer to $\Delta_f H_{298}^\circ$ values in kcal mol^{-1} derived from the CBS-QB3 calculations. The complete set of computational results is available from the authors upon request.

3. Results and discussion

3.1. Identification of the ionic dissociation products of metastable 2-aminoxyethanol ions

The 70 eV mass spectrum of 2-aminoxyethanol is shown in Fig. 1a. A weak molecular ion signal is observed at *m*/*z* 77. Pseudo direct bond cleavage in the molecular ion leads to the base peak at *m*/*z* 45 corresponding to CH_3CHOH^+ [3] (direct bond cleavage into $^+CH_2CHOH$ is not an option: this ion is not a minimum on the $C_2H_5O^+$ potential energy surface). Losses of $NH_2^\bullet$ and NH_3 lead to the low intensity peaks at *m*/*z* 60 and 61. The signals at *m*/*z* 31 (CH_2OH^+) and 29 (HCO^+), characteristic of ions having primary hydroxyl functionalities, result from carbon–carbon bond cleavage. The complementary reaction, resulting from $CH_2OH^\bullet$ loss, rationalizes the weak signal at *m*/*z* 46. By analogy with ionized 1,2-ethanediol [4], a double hydrogen transfer reaction could take place to generate protonated methanol at *m*/*z* 33. However, a high-resolution GC–MS experiment shows that the *m*/*z* 33 ions are $[N,H_3,O]^{\bullet+}$ ions and that they do not originate from a contaminant.

On the other hand, the metastable ion (MI) spectrum of $NH_2OCH_2CH_2OH^{\bullet+}$ is dominated by a different set of reactions. As shown in Fig. 1b, substantial signals at *m*/*z* 61, 60, 46, 32 and 18 are observed along with a much less intense *m*/*z* 47 peak. The *m*/*z* 45 signal, which is the base peak in the 70 eV EI mass spectrum and also the CID mass spectrum (Fig. 1c), is absent in the MI spectrum.

Structure assignments of the product ions produced in the above low-energy dissociations follow from the analysis of our tandem mass spectrometry results, that is from the high-energy CID mass spectra of ions dissociating in the metastable timeframe [3].

The CID mass spectrum of the *m*/*z* 61 product ions is shown in Fig. 1e. This spectrum is compatible with that of carbonyl-protonated glycolaldehyde ions $HOCH_2CH(OH)^+$ (**1**a): it closely resembles that of the *m*/*z* 61 ions generated by loss of $HCO^\bullet$ from ionized glyceraldehyde, $HOCH_2CH(OH)CHO^{\bullet+}$. Further support for this assignment comes from a detailed experimental and computational study of protonated glycolaldehyde [14], which inter alia provides a convincing rationale for the intense water loss peak at *m*/*z* 43 ($CH_3C{=}O^+$) in the CID mass spectrum.

Analysis of the CID spectrum of Fig. 1f leads to the proposal that the *m*/*z* 60 ions of the MI spectrum represent a 3:1 mixture of ionized glycolaldehyde, $HOCH_2C(=O)H^{\bullet+}$ (**2**a), and dihydroxyethene, $HOC(H){=}C(H)OH^{\bullet+}$ (**2**b). This assertion is based upon a careful comparison with the reference spectra available in the literature [3,15a,d]. The spectrum of Fig. 1f is close to that of ionized glycolaldehyde and features a narrow peak at *m*/*z* 32 for its decarbonylation into $CH_2OH_2^{\bullet+}$ [15b,c]. On the other hand, loss of water does not occur from **2**a and the broadened peak at *m*/*z* 42 characterizes the presence of enol ions **2**b.

Fig. 1g shows the CID mass spectrum of the *m*/*z* 47 product ion generated by loss of CH_2O. This spectrum is not compatible with that of ionized *N*- or *O*-methylhydroxylamine for which reference spectra are available [16a]. We propose that it corresponds to $HC(OH)NH_3^{\bullet+}$ (**3**a), an ylide ion that has not previously been characterized experimentally. The exothermicity of its generation, see Scheme 1, makes it an attractive proposal.

The CID mass spectrum of Fig. 1h clearly represents [16b] that of *m*/*z* 46 ions having the structure of carbonyl-protonated formamide, $HC(OH)NH_2^+$ (**4**a). The spectra of the *m*/*z* 18 and 32 ions (not shown) are in excellent agreement with those of NH_4^+ and the well-characterized methylene oxonium ion $CH_2OH_2^{\bullet+}$ [3].

Scheme 1 summarizes the above ion structure assignments and lists the thermochemical energy requirement for the various reactions. Also given are the kinetic energy releases derived from the metastable peaks ($T_{0.5}$ values in meV). Their relatively high values suggest that the reactions do not take place at the thermochemical threshold [3]. We further note that lack of sen-

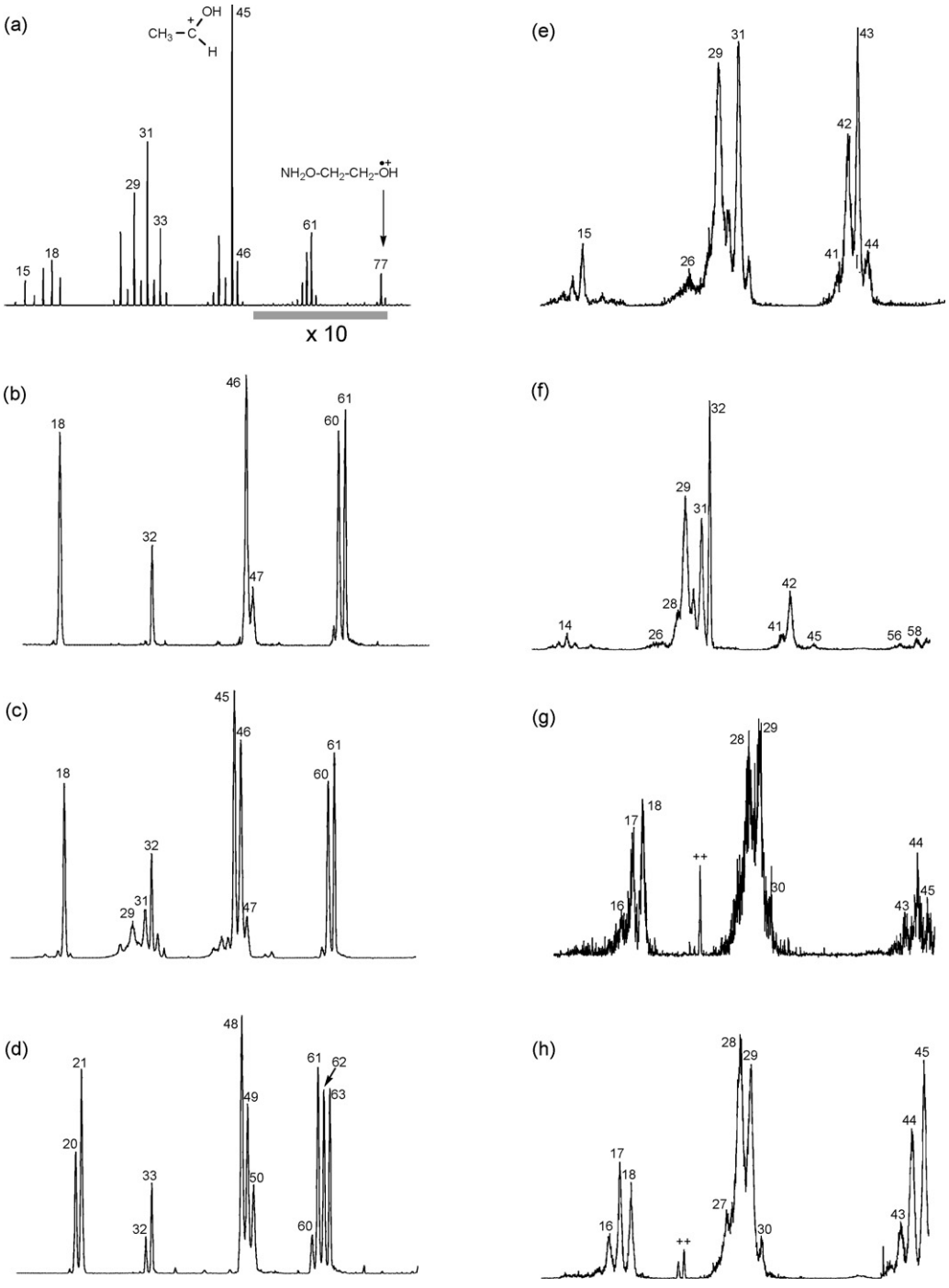

Fig. 1. (a) Seventy electron volt EI mass spectrum of $NH_2OCH_2CH_2OH$ (2-aminoxyethanol); the MI and CID spectra of the molecular ion are represented by items (b) and (c), respectively; whereas item (d) shows the MI spectrum of $ND_2OCH_2CH_2OD^{\bullet+}$; items (e)–(h) are CID spectra of, respectively, *m/z* 61, 60, 47 and 46 ions generated from metastable ions $NH_2OCH_2CH_2OH^{\bullet+}$.

sitivity prevented us to use the CIDI technique [3] to probe the identity of the neutral species lost in the generation of the *m/z* 32 and *m/z* 18 ions.

3.2. The energy requirement for dissociating metastable 2-aminoxyethanol ions

The generation of *m/z* 45 ions CH_3CHOH^+ is the predominant reaction among source-generated ions, but it is absent among the dissociating metastable ions. The reaction likely involves the pseudo direct bond cleavage reaction of Scheme 1, which is calculated to lie at 171 kcal mol^{-1}. In the absence of energetic information from appearance energies, we propose as an alternative criterion that the calculated mechanistic proposals for the dissociation chemistry of metastable 2-aminoxyethanol ions are viable only if their energy requirement lies below that of the above pseudo direct bond cleavage at 171 kcal mol^{-1}.

Table 1
Energetic data derived from CBS-QB3 calculations of stable isomers and connecting transition states involved in the dissociation chemistry of ionized 2-aminoxyethanol (AE-1)[a]

Ionic species	B3LYP/CBSB7 *E* (total)	CBS-QB3 *E* (total) (0 K)	**ZPE**	QB3 $\Delta_f H_0^\circ$	QB3 $\Delta_f H_{298}^\circ$	$\langle S^2 \rangle$
AE-1a (Scheme 1)	−285.34536	−284.82107	63.3	143.9	137.5	0.77
AE-1b (Scheme 3a)	−285.32671	−284.80312	62.7	155.2	149.3	0.77
AE(N)-1 (Fig. 2a)	−285.63142	−285.12150	63.4	−44.6	−50.7	–
AE(N)-2 (Fig. 2a)	−285.63745	−285.12518	63.8	−46.9	−53.3	–
AE-2 (Scheme 2)	−285.31049	−284.78503	63.3	166.5	160.0	0.76
AE-3a (Scheme 3a)	−285.33139	−284.81028	63.5	150.7	144.6	0.76
AE-3b (Scheme 3a)	−285.32185	−284.80118	63.3	156.4	150.4	0.76
AE-3b$_1$ (Scheme 3a)	−285.31859	−284.79577	62.6	159.8	154.1	0.77
AE-4 (Scheme 3b)	−285.37330	−284.85345	62.8	123.6	117.4	0.77
TS AE 1a → 1b	−285.32327	−284.80272	62.3	155.4	149.2	0.77
TS AE 1a → 2	−285.30154	−284.77520	60.7	172.7	165.8	0.76
TS AE 1a → 3b	−285.30193	−284.78040	61.0	169.4	162.6	0.78
TS AE 1b → 3a	−285.30655	−284.78467	61.0	166.8	160.0	0.79
TS AE 3a → 3b	−285.31706	−284.79807	62.5	158.4	152.0	0.76
TS AE 3b → 3b$_1$	−285.31658	−284.78909	62.4	164.0	158.1	0.78
IDC-1 (Scheme 3a)	−285.34494	−284.81562	61.1	147.3	142.0	0.77
IDC-2 (Scheme 2)	−285.36316	−284.83185	58.0	137.2	132.8	0.77
TS AE 2 → IDC-2	−285.29012	−284.76615	59.3	178.4	172.3	0.76
TS AE 3b$_1$ → IDC-1	−285.31837	−284.79414	62.0	160.8	154.9	0.77
HBRC-1 (Scheme 3a)	−285.33748	−284.81701	59.9	146.5	141.2	0.76
HBRC-2 (Scheme 3a)	−285.35486	−284.83549	59.2	134.9	129.0	0.76
HBRC-3a (Scheme 3b)	−285.38561	−284.85707	60.5	121.3	116.0	0.76
HBRC-3b (Scheme 3b)	−285.36620	−284.84980	58.4	125.9	120.3	0.76
HBRC-4 (Scheme 3b)	−285.39749	−284.87845	58.1	107.9	104.3	0.76
HBRC-5 (Scheme 3b)	−285.41128	−284.88688	60.9	102.6	97.5	0.76
HBRC-6 (Scheme 3b)	−285.38726	−284.86617	61.3	115.6	110.7	0.76
$[CH_2–O–N(H)\cdots H\cdots O(H)CH_2]^{\bullet+}$	−285.27300	−284.74215	59.2	193.4	189.0	0.76
$[CH_2–O–N(H_2)\cdots H\cdots O{=}CH_2]^{\bullet+}$	−285.30503	−284.78464	59.9	166.8	161.9	0.76
TS IDC 1 → HBRC 1	−285.33458	−284.82069	58.4	144.2	138.5	0.76
TS HBRC 1 → 2	−285.33208	−284.81267	59.6	149.2	143.7	0.76
TS HBRC 2 → 3b	−285.35363	−284.83649	57.4	134.2	128.5	0.76
TS HBRC 2 → 5	−285.34207	−284.82498	59.7	141.5	135.8	0.76
TS HBRC 3b → 3a	−285.36530	−284.83883	59.0	132.8	127.5	0.76
TS HBRC 3a → 4	−285.37314	−284.83722	59.8	133.8	128.3	0.81
TS HBRC 5 → 6	−285.36445	−284.83851	58.4	133.0	127.5	0.76
IDC-3 (Scheme 5)	−285.37067	−284.83880	59.8	132.8	127.4	0.77
IDC-4a (Scheme 5)	−285.40272	−284.87498	61.8	110.1	105.0	0.76
IDC-4b (Scheme 5)	−285.40844	−284.87961	62.1	107.2	102.0	0.76
HBRC-7 (Scheme 5)	−285.43833	−284.91141	62.0	87.2	81.6	0.81
HBRC-8 (Scheme 5)	−285.34267	−284.82347	59.0	142.4	137.5	0.76
TS HBRC 8 → IDC-4b	−285.33502		56.9	148.5	143.1	0.76

[a] $E_{(total)}$ in Hartrees, all other components, including the ZPE scaled by 0.99, are in kcal mol^{-1}.

The activation energy for this process, relative to the lowest energy conformer **AE-1a**, is significant (33 kcal mol^{-1}, see Scheme 1) and leads one to expect that 2-aminoxyethanol would exhibit a sizeable molecular ion signal in its EI mass spectrum. This is clearly not the case, see Fig. 1a, and the following provides a rationale. First we note that neutral 2-aminoxyethanol possesses a great many conformational isomers. Of these, the two "*cis*" isomers of Fig. 2 are the most stable because of internal hydrogen-bridges (the "*cis*/*trans*" annotation refers to the relative position of the hydroxyl and the aminoxy groups). The lowest energy conformer **AE(N)-2** is internally hydrogen-bridged with the hydroxyl hydrogen acting as the bridging hydrogen. The other conformer, **AE(N)-1**, whose bridging hydrogen belongs to the aminoxy functional group, lies 2.6 kcal mol^{-1} higher in energy. Thus, if one assumes that an equilibrium exists between these conformers prior to ionization, almost all of the incipient ions are formed from neutrals having the structure of **AE(N)-2**. Our calculations indicate that the vertical ionization energy of **AE(N)-2** is 9.27 eV and that the ion is not a minimum on the potential energy surface: it optimizes to ion **AE-1a**. This scenario predicts that EI generates **AE-1a** ions having 22 kcal mol^{-1} of excess internal energy. These ions require a mere 11 kcal mol^{-1} of energy to dissociate into *m*/*z* 45 ions and this may well explain the low intensity of the molecular ion signal.

3.3. The dissociation mechanisms for metastable 2-aminoxyethanol ions: does its dissociation chemistry resemble that of ionized 1,2-ethanediol?

In this and the following sections, we present the results of our CBS-QB3 computational analysis of the mechanisms by which metastable aminoxyethanol ions dissociate. Previous work [3,4] has shown that metastable 1,2-ethanediol ions dissociate via the hydrogen-bridged intermediate, $CH_2O(H)\cdots H\cdots O{=}CH_2^{\bullet+}$. Therefore, we first examined the possibility that the metastable 2-aminoxyethanol ions isomerize into the two hydrogen-bridged analogues as shown in Scheme 2.

Their generation may be envisaged to occur via carbon–carbon bond cleavage of ions **AE-1a**. In HBRC $[CH_2{-}O{-}N(H)\cdots H\cdots O(H)CH_2]^{\bullet+}$ the bridging H atom is donated by the NH_2O group, whereas it originates from the OH group in its isomer $[CH_2{-}O{-}N(H_2)\cdots H\cdots O{=}CH_2]^{\bullet+}$.

The calculated enthalpies of formation for the two species are 189 and 162 kcal mol^{-1}, respectively. This implies that the ion $[CH_2{-}O{-}N(H)\cdots H\cdots O(H)CH_2]^{\bullet+}$ does not play a role in the dissociation chemistry as it lies higher in energy than the 1,2-*H* shift transition state that yields the *m*/*z* 45 ion. The enthalpy of $[CH_2{-}O{-}N(H_2)\cdots H\cdots O{=}CH_2]^{\bullet+}$ is not too high to discount it as a possible intermediate, but our calcu-

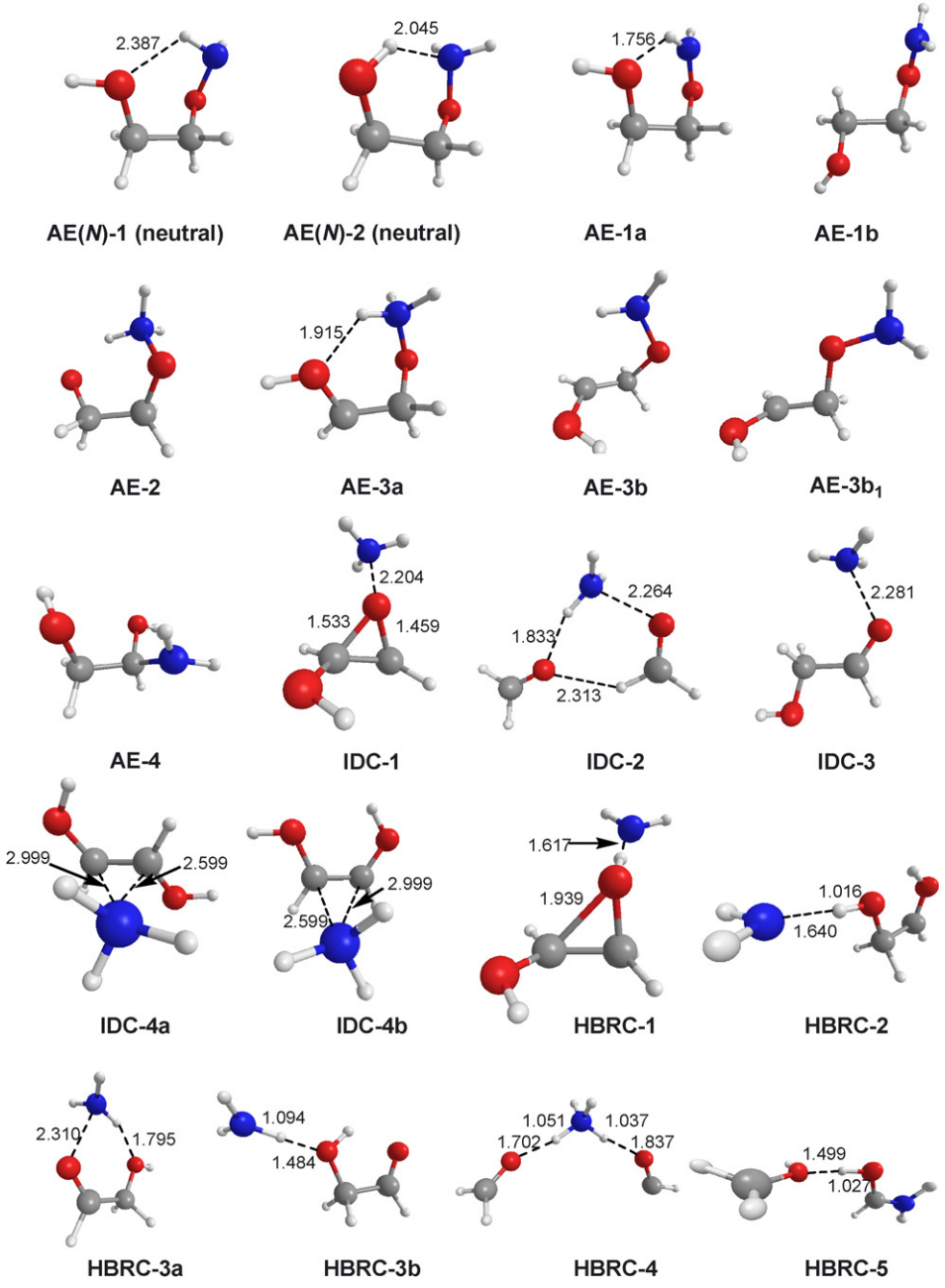

Fig. 2. Selected optimized geometries (CBSB7 basis set) for stable intermediates and connecting transition states involved in the dissociation chemistry of ionized 2-aminoxyethanol (**AE-1**).

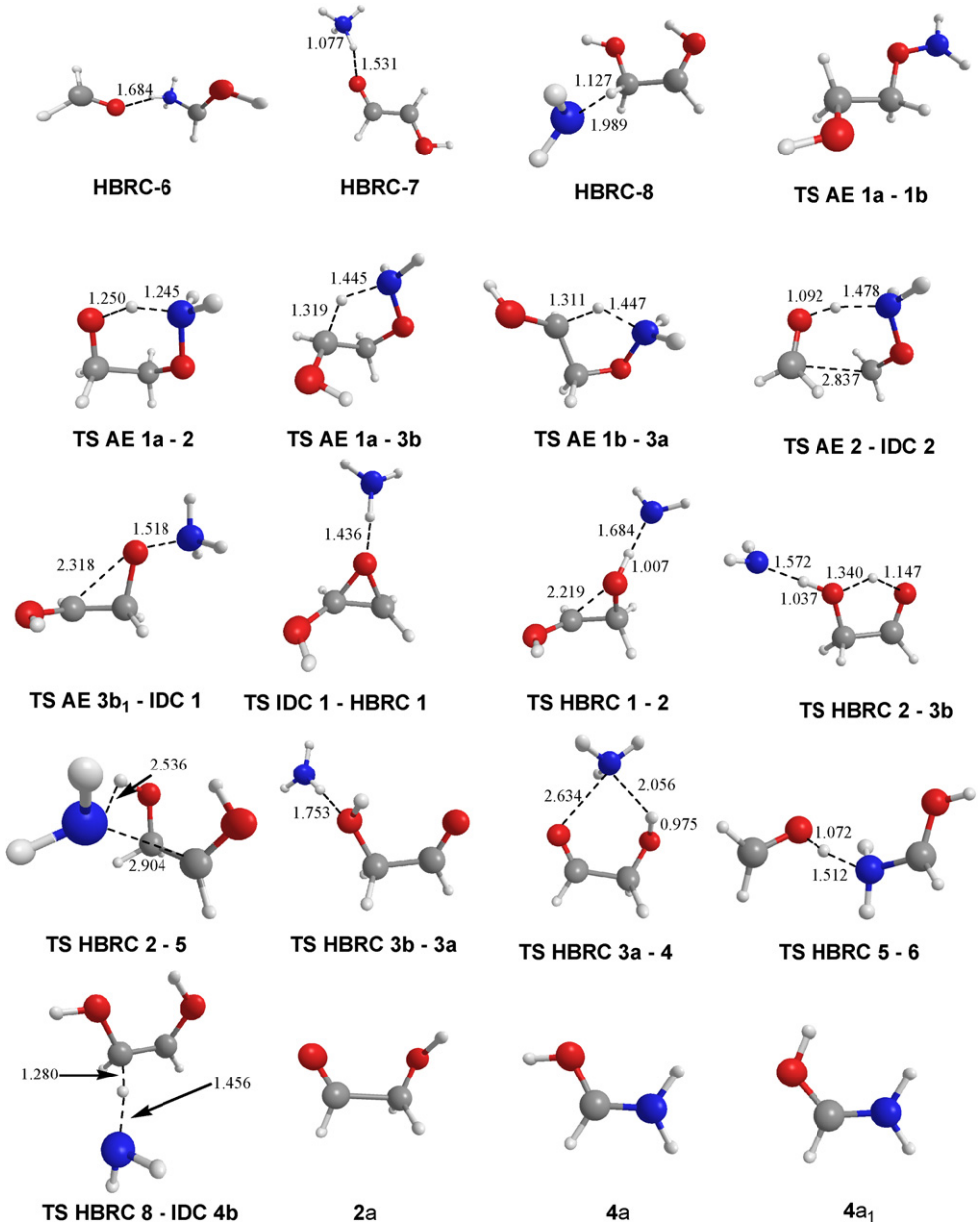

Fig. 2. (*Continued*).

lations indicate that the process by which it is generated is too energy demanding. As shown in Scheme 2, ion **AE-1a** first rearranges by a 1,5-*H* shift into the distonic ion **AE-2**, which further rearranges into the HBRC by fission of its carbon–carbon bond. The overall energy requirement for this transformation lies at 172 kcal mol^{-1}, slightly above the energy criterion of Section 3.1. We further note that ions having the structure $CH_2ONH_3^{\bullet+}$ are expected to exothermically dissociate

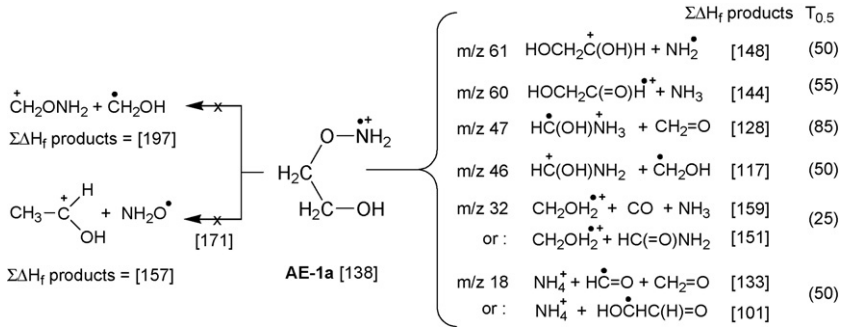

Scheme 1.

Table 2
Energetic data for various dissociation products of ionized 2-aminoxyethanol derived from CBS-QB3 and selected CBS-APNO calculations[a]

Species		*m/z*	CBS-QB3 *E* (total) (0 K)	QB3 $\Delta_f H_0^\circ$	QB3 $\Delta_f H_{298}^\circ$	APNO $\Delta_f H_{298}^\circ$	Expt. $\Delta_f H_{298}^\circ$	Ref./note
$HOCH_2CH(OH)^+ + NH_2^\bullet$	**1**a	61		152	**148**	**147**	–	
$HOCH_2CH(OH)^+$	**1**a		−229.01653	106.6	102.6	102.4	–	b
$HC(=O)CH_2OH_2^+$	**1**b		−229.00695	112.6	108.3	107.9	–	b
$NH_2^\bullet$			−55.79117	45.7	45.1	44.9	45	c
$HOCH_2C(=O)H^{\bullet+} + NH_3$	**2**a	60		149	**144**	**143**	**–**	
$HOC(H)=C(H)OH^{\bullet+} + NH_3$	**2**b	60		119	**114**	**113**	**112**	
$HOCH_2C(=O)H^{\bullet+}$	**2**a		−228.35314	157.6	154.8	154.0		d
$HOC(H)=C(H)OH^{\bullet+}$ (*cis*)	**2**b		−228.40028	128.0	124.6	124.0	123	e
$HOC(H)=C(H)OH^{\bullet+}$ (*trans*)			−228.39561	130.9	127.7	126.9	–	f
$OCH_2C(H)OH^{\bullet+}$	**2**c		−228.33339	170.0	166.6	166.5	–	g
$CH_2OC(H)OH^{\bullet+}$	**2**d		−228.36750	148.6	145.4	145.0	–	
NH_3			−56.46019	−8.8	−10.5	−10.8	−11	c
TS AE-3b → *m/z* 60 (**2**a)			−284.81374	168.2	162.2	–	–	
$HC(OH)NH_3^{\bullet+} + CH_2O$	**3**a	47		133	**128**	**128**	–	
$HC(OH)NH_3^{\bullet+}$	**3**a		−170.49411	159.5	155.4	154.7	–	
CH_2O			−114.34411	−26.4	−27.3	−26.6	−26	c
$HC(OH)NH_2^+ + CH_2OH^\bullet$	**4**a	46		122	**117**	**116**	**121**	h
$HC(OH)NH_2^+$	**4**a		−169.96749	124.7	121.1	120.9	125	d,i
	4a$_1$		−169.96227	128.0	124.4	124.1	–	d
$CH_2ONH_2^+$	**4**b		−169.83951	205.0	201.7	202.6	–	
$CH_2OH^\bullet$			−114.88817	−2.5	−4.2	−5.2	−4	j
$CH_3C(H)OH^{\bullet+} + NH_2O^\bullet$		45		161	**157**	**157**	–	
TS AE-1 → $CH_3C(H)OH^{\bullet+}$		45	−284.77013	175.9	170.6	–	–	
$CH_3C(H)OH^{\bullet+}$			−153.87252	145.7	142.2	141.1	139	h
$NH_2O^\bullet$			−130.92056	15.8	14.3	15.4	–	
$CH_2OH_2^{\bullet+} + CO + NH_3$		32		162	**159**	**158**	**158**	
$CH_2OH_2^{\bullet+} + HC(=O)NH_2$		32		155	**151**	**150**	**151**	
$CH_2OH_2^{\bullet+}$			−115.14931	198.9	196.5	195.3	195	h
CO			−113.18197	−27.7	−26.9	−26.4	−26.5	c
$HC(=O)NH_2$			−169.65355	−43.6	−46.0	−45.3	−44	c
$NH_4^+ + HCO^\bullet + CH_2O$		18		137	**133**	**134**	**136**	
$NH_4^+ + HC(=O)CHOH^\bullet$		18		107	**101**	**101**	–	
NH_4^+			−56.78320	153.8	151.1	150.6	151	c
$HCO^\bullet$			−113.70496	9.4	9.5	9.6	10	j
$HC(=O)CHOH^\bullet$			−228.09740	−47.2	−49.7	−49.6	–	

Bold numbers represent the sum of the enthalpies of formation for various dissociation products.
[a] $E_{(total)}$ in Hartrees, all other components, including the ZPE scaled by 0.99, are in kcal mol^{-1}.
[b] Calculation refers to the most stable conformer as reported in ref. [14].
[c] Ref. [19a].
[d] Calculation refers to the conformer shown in Fig. 2.
[e] From ref. [19a] but using IE = 8.62 eV, not 9.62 eV (misprint).
[f] Calculation refers to the conformer of Scheme 5.
[g] Calculation refers to the conformer of Scheme 4.
[h] Experimental value from ref. [3].
[i] Experimental value from ref. [3], which uses −44.5 kcal mol^{-1} as the 298 K enthalpy of formation of formamide from ref. [19c]; the CBS-QB3 and CBS-APNO values are −46.0 and −45.3 kcal mol^{-1}, respectively.
[j] Ref. [19b].

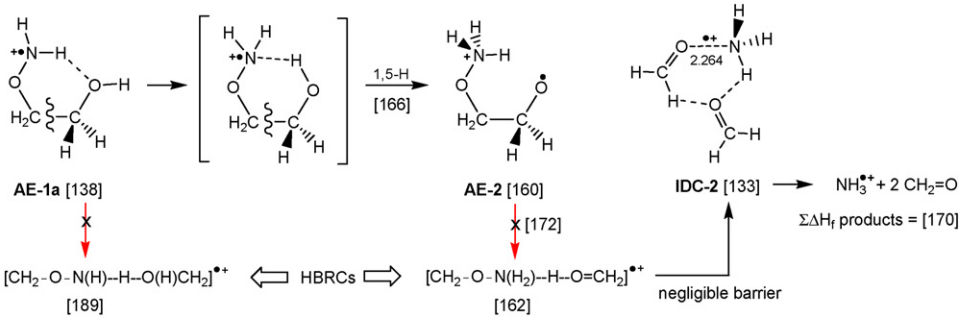

Scheme 2.

by loss of CH_2O [16]. Thus it is not surprising that the calculation indicates that the CH_2ONH_3 component of the HBRC $[CH_2–O–N(H_2)\cdots H\cdots O{=}CH_2]^{\bullet+}$ triggers a facile conversion to the energetically more attractive *ter*-body complex **IDC-2**. However, incipient **IDC-2** ions generated by the route of Scheme 2 have some 40 kcal mol^{-1} of internal energy, more than enough for a rapid dissociation into $NH_3^{\bullet+} + 2CH_2{=}O$. It is conceivable that NH_4^+ ions are co-generated in this process but, as shown in Section 3.4, a pathway of much lower energy is available for this reaction.

3.4. The dissociation mechanisms for metastable 2-aminoxyethanol ions: losses of $NH_2^{\bullet}$, NH_3, and the generation of NH_4^+

The first step of all of our mechanistic proposals for the dissociation of metastable 2-aminoxyethanol ions **AE-1** is the 1,4-*H* shift leading to **AE-3b** depicted in Scheme 3a.[1] This step appears to be less energy demanding than the 1,5-*H* shift leading to ion **AE-2** of Scheme 2. It reflects the finding that ion **AE-3b** is more stable than ion **AE-2**.

The transformation **AE-1a** → **AE-3b** lies at 163 kcal mol^{-1}. However, a more circuitous route involving the rotational conformer **AE-3a**, *viz.*, **AE-1a** → **AE-1b** → **AE-3a** → **AE-3b** is 3 kcal mol^{-1} less energy demanding. Ion **AE-3b** can easily generate its rotational conformer **AE-3b$_1$**, which subsequently rearranges into **IDC-1**. This rearrangement involves elongation of the nitrogen–oxygen bond in concert with the formation of a bond between the aminoxy oxygen atom and the hydroxyl-substituted carbon atom. The resulting ion, **IDC-1**, can be viewed as an ion–dipole complex between a substituted oxirane ion and NH_3. An ensuing barrierless H atom transfer yields the protonated oxirane complex **HBRC-1** which can ring open with a negligible barrier into **HBRC-2**.

Fig. 2 shows that the more heavily substituted carbon atom of **HBRC-1** possesses an unusually long bond (1.9 Å) with the protonated oxirane oxygen atom. A recent computational study [17] suggests that DFT methods underestimate the strength of the C–O bond of such species and further recommends the use of CCSD derived geometries. We therefore performed a geometry optimization of **HBRC-1** using the more sophisticated QCISD/6-311G(d,p) level of theory. At this level of theory **HBRC-1** is not even a minimum and its optimized geometry is that of **HBRC-2** supporting the proposal that C–O bond cleavage in **HBRC-1** involves no significant barrier.

Loss of $NH_2^{\bullet}$ from **HBRC-2** may well account for the abundant production of protonated glycolaldehyde (*m/z* 61 in Fig. 1b). As shown in Scheme 3b, the other dissociation processes also involve **HBRC-2** as a key intermediate.

A hydrogen transfer to its $NH_2^{\bullet}$ component in concert with a 1,4-*H* shift in the incipient glycolaldehyde component leads to **HBRC-3b**, which can be viewed as an ionized glycolaldehyde–NH_3 complex. The incipient **HBRC-3b** ions may lose NH_3 to yield ionized glycolaldehyde, or rearrange further via carbon–carbon bond cleavage into the *ter*-body complex **HBRC-4**. Ions **HBRC-4** generated from **AE-1** have a very high internal energy content (>56 kcal mol^{-1}, see the dashed line in Scheme 3b) and will therefore rapidly decompose into NH_4^+ by the consecutive loss of $HCO^{\bullet} + CH_2{=}O$.

For the loss of NH_3 we have also considered the three pathways depicted in Scheme 4.

(i). The incipient ions **AE-3b** generated by a 1,4-*H* shift at 160 kcal mol^{-1} can be envisaged to undergo direct bond cleavage into the $C_2H_4O_2^{\bullet+}$ isomer **2c** and NH_3; the calculated minimum energy requirement for this reaction is 157 kcal mol^{-1}. Our calculations also indicate that upon extension of the nitrogen–oxygen bond in **AE-3b**, a 1,4-*H* shift may occur in concert yielding ionized glycolaldehyde and NH_3. However, neither of these routes is expected to effectively compete with the energetically much more attractive pathway of Scheme 3a and b.

(ii). Ions **IDC-1** of Scheme 3a may be envisaged to undergo the C–C bond cleavage depicted on the right hand side of Scheme 4. This would lead to the formation of the $C_2H_4O_2^{\bullet+}$ isomer **2**d, a stable distonic ion whose dissociation chemistry has been studied in detail [15d,e] in conjunction with that of its 1,4-*H* shift isomer ionized methyl formate [15f]. From an energetic point of view this route cannot be excluded: a potential energy surface scan (at the B3LYP/CBSB7 level of theory) of **IDC-1** involving elongation of the C–C bond indicates that at 1.86 Å, the reaction goes through a maximum at 157 kcal mol^{-1}. However, upon further elongation of the bond an exothermic concerted proton transfer occurs leading to $[CH_2–O–C(H){=}O\cdots H\cdots NH_3]^{\bullet+}$, an intermediate HBRC of **2**d and NH_3, which easily rearranges into the *ter*-body complex **HBRC-4** discussed above, see Scheme 3b. Thus, the C–C bond cleavage of Scheme 4, if it occurs at all, is not expected to yield the distonic ion **2**d but rather **HBRC-4**s dissociation products $NH_4^+ + CH_2{=}O + HCO^{\bullet}$.

Experiment supports this proposal: the CID mass spectrum of Fig. 1f does not contain the tell-tale peak at *m/z* 45 indicative of the presence of the distonic ion **2**c or its isomer ionized methylformate [15d].

As discussed in Section 3.1, our experiments indicate that c. 25% of the $C_2H_4O_2^{\bullet+}$ ions generated by loss of NH_3 are not glycolaldehyde ions $HOCH_2C(=O)H^{\bullet+}$ (**2**a) but rather their more stable enol isomer $HOC(H){=}C(H)OH^{\bullet+}$ (**2**b). The enol ions cannot be generated from solitary glycolaldehyde ions: the fairly low-energy requirement for the decarbonylation of **2**a into $CH_2OH_2^{\bullet+}$ (15 kcal mol^{-1}) [15b,c] prohibits isomerization into **2**b by a 1,3-*H* shift (32 kcal mol^{-1}, this work). However, the co-generation of **2**b can readily be rationalized if a catalysed transformation of **2**a is invoked.

[1] A reviewer has suggested that O–N bond cleavage in **AE-1** followed by a delayed (hidden) 1,3-*H* shift could account for the $NH_2^{\bullet}$ loss. Our calculations indicate that this is not a viable option: the $HOCH_2CH_2O^+$ product ion is not a minimum and elongation of the O–N bond leads to the ter–body complex $[CH_2{=}O\cdots NH_3\cdots O{=}CH_2]^{\bullet+}$ with an energy requirement of 48 kcal mol^{-1}. A direct 1,3-*H* shift to the ONH_2 moiety does not initiate loss of $NH_2^{\bullet}$ either: this reaction would generate $CH_2{=}CH–OH^{\bullet+} + NH_2OH$, via a prohibitively high barrier of 50 kcal mol^{-1}.

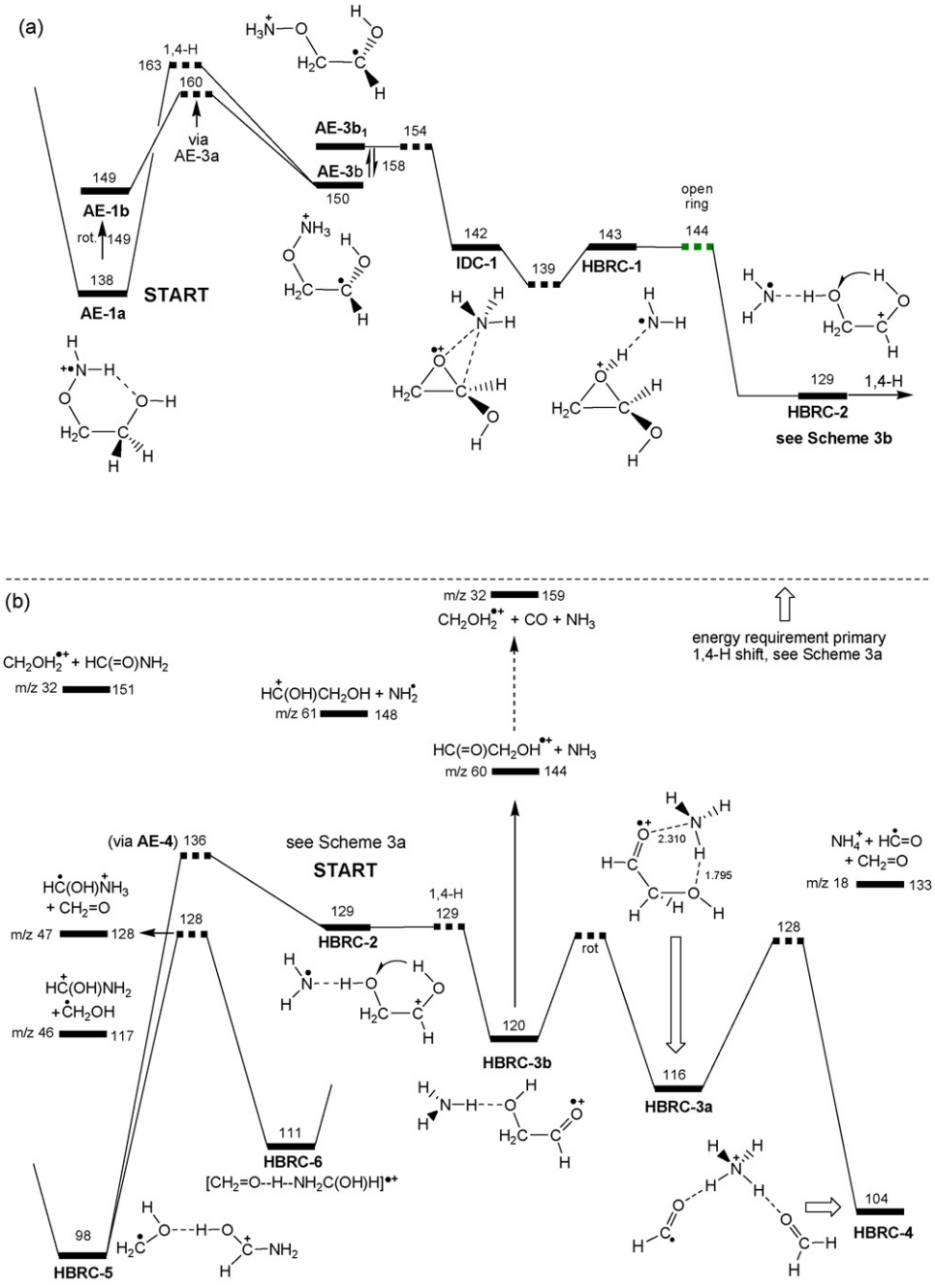

Scheme 3.

In proton-transport catalysis, a base molecule abstracts a proton from its ionic partner, and subsequently back donates the proton to an alternative acceptor site on the ion [5]. In line with the pioneering computational studies of Gauld and Radom [18], this process is most efficient when the base molecule's proton affinity lies between the proton affinities of the donor and acceptor sites of the associated radical.

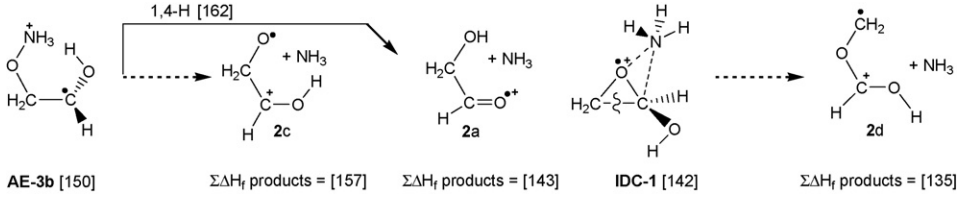

Scheme 4.

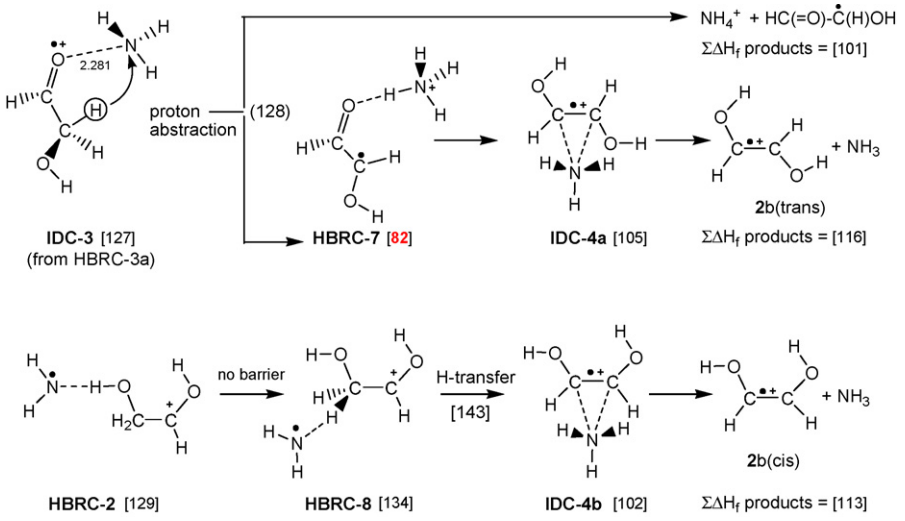

Scheme 5.

We propose that NH_3 acts as the base in the proton-transport catalysis mechanism depicted in the top part of Scheme 5. The first step involves the barrierless abstraction of the methylene proton by the base in the ion–dipole complex **IDC-3**, which can readily be generated from the **HBRC-3a** ions depicted in Scheme 3b.

The resulting ammoniated complex, **HBRC-7**, is very stable, having an enthalpy of formation of only 82 kcal mol^{-1}. Back-donation of the proton to the oxygen atom yields **IDC-4a**, which can be viewed as an ionized 1,2-dihydroxyethene–NH_3 complex. We note that in this catalysed transformation, the proton affinity of the base, NH_3, is higher than the proton affinity of the acceptor site of the radical, HC(–O$^\bullet$)=CHOH. This is reflected on the difference in threshold energies for the generation of the dissociation products, $NH_4^+ + HC(=O)–CHOH^\bullet$ at 101 kcal mol^{-1} and $HOC(H)=C(H)OH^{\bullet+} + NH_3$ at 114 kcal mol^{-1}. Since ions **HBRC-7** generated from **AE-1** are energy rich, their dissociation may account for the generation of ions **2**b by proton-transport catalysis and also contribute to the formation of NH_4^+ ions.

The bottom part of Scheme 5 depicts an alternative pathway for the conversion **2**a → **2**b. In it the $NH_2^\bullet$ component of **HBRC-2** migrates to the methylene group to form **HBRC-8**. The subsequent abstraction of the methylene hydrogen atom leads to the formation of **IDC-4b**, a rotational isomer of the ionized 1,2-dihydroxyethene–NH_3 complex, which dissociates into the *trans* isomer of **2**b. This route is less attractive because its overall energy requirement (143 kcal mol^{-1}) is considerably higher than that for the proton-transport catalysis discussed above.

3.5. The dissociation mechanisms for metastable 2-aminoxyethanol ions: losses of CH_2O, $CH_2OH^\bullet$ and the generation of $CH_2OH_2^{\bullet+}$

As shown in Scheme 3b, the *m/z* 32, 46, and 47 ions also originate from rearrangement processes initiated in the **HBRC-2** ion. The $NH_2^\bullet$ radical can migrate to the aldehyde carbon atom via a connecting transition state at 136 kcal mol^{-1}. The resulting covalently bound structure, **AE-4**, is not very stable and easily rearranges into the hydrogen-bridged ions **HBRC-5/6**. Loss of the $CH_2OH^\bullet$ component of **HBRC-5** yields the observed protonated formamide, whereas **HBRC-6** readily generates the *m/z* 47 ion $HC(OH)NH_3^{\bullet+}$ by loss of its CH_2=O component.

Proton abstraction by the $CH_2OH^\bullet$ moiety of **HBRC-5** would yield the $CH_2OH_2^{\bullet+}$ ion at *m/z* 32. However, this process is 34 kcal mol^{-1} higher in energy than the simple bond cleavage of the **HBRC-5** complex into $CH_2OH^\bullet + HC(OH)NH_2^+$. This makes it unlikely that **HBRC-5** acts as a major precursor for the generation of $CH_2OH_2^{\bullet+}$. A more plausible route, see Scheme 3b, involves the decarbonylation of the energy rich fraction of the incipient glycolaldehyde ions generated from **HBRC-3a/b**. This decarbonylation has been studied before by experiment and theory [15b,c] and appears to occur at the thermochemical threshold. This threshold lies at 159 kcal mol^{-1}, slightly below the energy requirement for the primary 1,4-*H* shift in **AE-1**.

3.6. Analysis of the deuterium-labelled isotopomer, $ND_2OCH_2CH_2OD^{\bullet+}$

Apart from the energy criterion discussed above, the proposed mechanisms must also satisfy the experimental observations of the D-labelled isotopomer $ND_2OCH_2CH_2OD$, whose MI spectrum is presented in Fig. 1d.

The proposals of Scheme 3a and b imply that ions **HBRC-2a** are initially generated with a D atom bonded to the carbonyl oxygen and two D atoms and one H atom in the $H_2N\cdots H\cdots O$ moiety of the complex. The H/D atoms of this moiety may rapidly exchange (via **HBRC-1** and **IDC-1**) so that the bridging atom becomes either H or D. Exchange reactions involving the CH_2 hydrogen atoms are unlikely: the primary 1,4-*H* shift leading to **AE-3b** is not expected to be reversible because all pathways leading therefrom are strongly exothermic.

This scenario accounts for the observed losses of ND_2H, $ND_2^{\bullet}$ and $NDH^{\bullet}$ as exemplified by the *m/z* 61–63 cluster of peaks in the MI spectrum. It also accounts for the cluster of peaks at *m/z* 48, 49 and 50: D-labelled $HC(OH)NH_2^+$ ions yield the peaks at *m/z* 48 and 49, while the $HC(OH)NH_3^{\bullet+}$ ions cleanly shift to *m/z* 50. In support of this interpretation we note that the peak intensity ratio (*m/z* 48 + *m/z* 49):*m/z* 50 is close to the *m/z* 46:*m/z* 47 ratio of the MI spectrum of the unlabelled compound.

The MI spectrum of Fig. 1d also displays a peak at *m/z* 60. This shows that to some extent the ammonia loss can also occur as ND_3. It suggests that the $ND_2^{\bullet}$ component of **HBRC-2** can also abstract, via a suitably oriented conformer, the D atom bonded to the carbonyl oxygen.

The peaks at *m/z* 21 and *m/z* 20 in the MI spectrum correspond to the D-labelled ammonium ions ND_3H^+ and $ND_2H_2^+$, respectively. The ND_3H^+ ion is the expected product ion from the route proposed in Scheme 3b, whereas $ND_2H_2^+$ could readily originate from the competing abstraction process presented in the top part of Scheme 5.

As discussed in Section 3.4, this route may also lead to proton-transport catalysis yielding ions $DOC(H)=C(H)OD^{\bullet+}$ and ions $HOC(H)=C(H)OD^{\bullet+}$. These are expected to contribute to the intensities of the *m/z* 61 and *m/z* 62 peaks in the MI spectrum. Since CID mass spectra of mixtures of partially labelled $C_2H_{4/5}O_2$ ions are very complex, we have not attempted to verify this interpretation by experiment.

The labelling results shed further light on the mechanisms of formation of the $CH_2OH_2^{\bullet+}$ ions discussed in the previous section. Dissociation of **HBRC-5**, by loss of formamide, is expected to yield both $CH_2OHD^{\bullet+}$ (*m/z* 33) and $CH_2OD_2^{\bullet+}$ (*m/z* 34) but a peak at *m/z* 34 is absent in the MI spectrum of Fig. 1d. Moreover this pathway cannot account for the presence of the peak at *m/z* 32 ($CH_2OH_2^{\bullet+}$). Our proposed route, involving decarbonylation of part of the incipient glycolaldehyde ions, provides a rationale: decarbonylation may occur from both *m/z* 60 ($HOCH_2C(=O)H^{\bullet+}$) and *m/z* 61 ($DOCH_2C(=O)H^{\bullet+}$) ions yielding the observed $CH_2OH_2^{\bullet+}$ (*m/z* 32) and $CH_2OHD^{\bullet+}$ (*m/z* 33) ions, respectively.

4. Summary

In this study we have examined the dissociation chemistry of low-energy 2-aminoxy-ethanol ions $NH_2OCH_2CH_2OH^{\bullet+}$ (**AE-1**) using tandem mass spectrometry in conjunction with deuterium labelling and computational chemistry.

In the microsecond timeframe, these ions spontaneously dissociate into the following ions: protonated glycolaldehyde (*m/z* 61, $HOCH_2CH(OH)^+$), ionized glycolaldehyde in admixture with its enol (*m/z* 60, $HOCH_2C(=O)H^{\bullet+}$ and $HOC(H)=C(H)OH^{\bullet+}$), protonated formamide (*m/z* 46, $HC(OH)NH_2^+$), the methylene oxonium ion (*m/z* 32, $CH_2OH_2^{\bullet+}$) and the ammonium cation (*m/z* 18, NH_4^+). The minor *m/z* 47 peak in the MI spectrum represents the generation of the distonic ion $HC(OH)NH_3^{\bullet+}$.

A mechanistic analysis based upon CBS-QB3 model chemistry calculations indicates that the distonic ion $NH_3OCH_2CHOH^{\bullet+}$ (**AE-3**) is a common intermediate in all dissociation pathways of **AE-1**. **AE-3** is generated from **AE-1** by a 1,4-*H* shift of moderate energy requirement. Once generated, ions **AE-3** readily isomerize into various interconverting hydrogen-bridged radical cations of which ionized glycolaldehyde–NH_3 complexes are key species. These complexes also account for the partial conversion of glycolaldehyde ions into their more stable enol counterpart by proton-transport catalysis.

Acknowledgements

J.K.T. thanks the Natural Sciences and Engineering Research Council of Canada (NSERC) for financial support. P.J.A.R. gratefully acknowledges financial support from The Netherlands Organization for Scientific Research. J.K.T. and K.J.J. gratefully acknowledge valuable discussions with Dr. P.C. Burgers (Erasmus University) as well as Drs. V.Y. Taguchi and M.A. Trikoupis (MOE). The synthetic efforts of Dr. Yie Xing in the synthesis of 2-aminoxyethanol are greatly appreciated.

References

[1] (a) S.D. Richardson, Trends Anal. Chem. 22 (2003) 666;
(b) S.D. Richardson, Anal. Chem. 74 (2002) 2719.
[2] V.Y. Taguchi, Rapid Commun. Mass Spectrom. 15 (2001) 455.
[3] J.L. Holmes, C. Aubry, P.M. Mayer, Assigning Structures to Ions in Mass Spectrometry, CRC Press, Boca Raton, 2007.
[4] P.J.A. Ruttink, P.C. Burgers, L.M. Fell, J.K. Terlouw, J. Phys. Chem. A 102 (1998) 176.
[5] (a) D.K. Bohme, Int. J. Mass Spectrom. Ion Process. 115 (1992) 95;
(b) C.Y. Wong, P.J.A. Ruttink, P.C. Burgers, J.K. Terlouw, Chem. Phys. Lett. 387 (2004) 204 (references cited therein).
[6] P.C. Burgers, J.K. Terlouw, in: N.M.M. Nibbering (Ed.), Encyclopedia of Mass Spectrometry, vol. 4, Elsevier, Amsterdam, 2005, p. 173.
[7] H.F. van Garderen, P.J.A. Ruttink, P.C. Burgers, G.A. McGibbon, J.K. Terlouw, Int. J. Mass Spectrom. Ion Process. 121 (1992) 159.
[8] J.L. Holmes, J.K. Terlouw, Org. Mass Spectrom. 15 (1980) 383.
[9] D. Dhanak, C.B. Reese, S. Romana, G. Zappia, J. Chem. Soc.: Chem. Commun. (1986) 903.
[10] J.A. Montgomery Jr., M.J. Frisch, J.W. Ochterski, G.A. Petersson, J. Chem. Phys. 112 (2000) 6532.
[11] J.W. Ochterski, G.A. Petersson, J.A. Montgomery Jr., J. Chem. Phys. 104 (1996) 2598.
[12] M.J. Frisch, G.W. Trucks, H.B. Schlegel, G.E. Scuseria, M.A. Robb, J.R. Cheeseman, J.A. Montgomery Jr., T. Vreven, K.N. Kudin, J.C. Burant, J.M. Millam, S.S. Iyengar, J. Tomasi, V. Barone, B. Mennucci, M. Cossi, G. Scalmani, N. Rega, G.A. Petersson, H. Nakatsuji, M. Hada, M. Ehara, K. Toyota, R. Fukuda, J. Hasegawa, M. Ishida, T. Nakajima, Y. Honda, O. Kitao, H. Nakai, M. Klene, X. Li, J.E. Knox, H.P. Hratchian, J.B. Cross, V. Bakken, C. Adamo, J. Jaramillo, R. Gomperts, R.E. Stratmann, O. Yazyev, A.J. Austin, R. Cammi, C. Pomelli, J.W. Ochterski, P.Y. Ayala, K. Morokuma, G.A. Voth, P. Salvador, J.J. Dannenberg, V.G. Zakrzewski, S. Dapprich, A.D. Daniels, M.C. Strain, O. Farkas, D.K. Malick, A.D. Rabuck, K. Raghavachari, J.B. Foresman, J.V. Ortiz, Q. Cui, A.G. Baboul, S. Clifford, J. Cioslowski, B.B. Stefanov, G. Liu, A. Liashenko, P. Piskorz, I. Komaromi, R.L. Martin, D.J. Fox, T. Keith, M.A. Al-Laham, C.Y. Peng, A. Nanayakkara, M. Challacombe, P.M.W. Gill, B. Johnson, W. Chen, M.W. Wong, C. Gonzalez, J.A. Pople, Gaussian 03 Revision C. 02, Gaussian, Inc, Wallingford CT, 2004.
[13] L.N. Heydorn, Y. Ling, G. de Oliveira, J.M.L. Martin, Ch. Lifshitz, J.K. Terlouw, Zeitschrift für Physikalische Chemie 215 (2001) 141.
[14] G. Bouchoux, F. Penaud-Berruyer, W. Bertrand, Eur. J. Mass Spectrom. 7 (2001) 351.

[15] (a) J.K. Terlouw, C.G. de Koster, W. Heerma, J.L. Holmes, P.C. Burgers, Org. Mass Spectrom. 18 (1983) 222;
(b) R. Postma, P.J.A. Ruttink, J.H. van Lenthe, J.K. Terlouw, Chem. Phys. Lett. 156 (1989) 245;
(c) H.K. Ervasti, P.J.A. Ruttink, in preparation;
(d) R. Flammang, M. Plisnier, G. Leroy, M. Sana, M.T. Nguyen, L.G. Vanquicken-borne, Chem. Phys. Lett. 186 (1991) 393;
(e) B.J. Smith, M.T. Nguyen, L. Radom, J. Am. Chem. Soc. 114 (1992) 1151;
(f) N. Heinrich, Th. Drewello, P.C. Burgers, J.C. Morrow, J. Schmidt, W. Kulik, J.K. Terlouw, H. Schwarz, J. Am. Chem. Soc. 114 (1992) 3776.
[16] (a) P.C. Burgers, C. Lifshitz, P.J.A. Ruttink, G. Schaftenaar, J.K. Terlouw, Org. Mass Spectrom. 24 (1989) 579;
(b) G. Schaftenaar, R. Postma, P.J.A. Ruttink, P.C. Burgers, G.A. McGibbon, J.K. Terlouw, Int. J. Mass Spectrom. Ion Process. 100 (1990) 521.
[17] P.R. Carlier, N. Deora, T. Crawford, J. Org. Chem. 71 (2006) 1592.
[18] J.W. Gauld, L. Radom, J. Am. Chem. Soc. 119 (1997) 9831.
[19] (a) S.G. Lias, J.E. Bartmess, J.F. Liebman, J.L. Holmes, R.O. Levin, W.G. Maillard, J. Phys. Chem. 17 (Suppl. 1) (1988) (Ref. Data);
(b) Y.-R. Luo, Handbook of Dissociation Energies in Organic Compounds, CRC Press, Boca Raton, 2003;
(c) NIST Chemistry WebBook, NIST Standard Reference Data Base Number 69, National Institute of Standards and Technology, Gaithersburg, MD, 2007.